

An In Vivo 3D Micro-CT Evaluation of Tooth Movement After the Application of Different Force Magnitudes in Rat Molar

Carmen Gonzales^a; Hitoshi Hotokezaka^b; Yoshinori Arai^c; Tadashi Ninomiya^d; Junya Tominaga^a; Insan Jang^a; Yuka Hotokezaka^e; Motohiro Tanaka^f; Noriaki Yoshida^g

ABSTRACT

Objective: To investigate the precise longitudinal change in the periodontal ligament (PDL) space width and three-dimensional tooth movement with continuous-force magnitudes in living rats.

Materials and Methods: Using nickel-titanium closed-coil springs for 28 days, 10-, 25-, 50-, and 100-g mesial force was applied to the maxillary left first molars. Micro-CT was taken in the same rat at 0, 1, 2, 3, 10, 14, and 28 days. The width of the PDL was measured in the pressure and tension sides from 0 to 3 days. Angular and linear measurements were used to evaluate molar position at day 0, 10, 14, and 28. The finite element model (FEM) was constructed to evaluate the initial stress distribution, molar displacement, and center of rotation of the molar.

Results: The initial evaluation of PDL width showed no statistical differences among different force magnitudes. Tooth movement was registered 1 hour after force application and gradually increased with time. From day 10, greater tooth movement was observed when 10 g of force was applied. The FEM showed that the center of rotation in the molar is located in the center of five roots at the apical third of the molar roots.

Conclusion: The rat's molar movement mainly consists of mesial tipping, extrusion of distal roots, intrusion of mesial root, palatal inclination, and mesial rotation. Although the initial tooth movement after the application of different force magnitudes until day 3 was not remarkably different, 10 g of force produced more tooth movement compared with heavier forces at day 28. (*Angle Orthod.* 2009;79:703–714.)

KEY WORDS: Tooth movement; In vivo micro-CT; FEM, Rat molar; Time lapse; Superimposition

INTRODUCTION

Orthodontic treatment is based on the principle that if prolonged force is applied to a tooth, tooth move-

ment will occur as the bone around the tooth remodels. As Proffit¹ stated, tooth movement is primarily a periodontal ligament (PDL) phenomenon since the bone response is mediated by the PDL.

The first histological reports on tooth movement in the early 20th century by Sandstedt² and Oppenheim³ included detailed drawings of histological slides because reproduction by photographs was not yet in use.⁴ Experiments performed on the responses of paradental tissues occurring incident to orthodontic tooth movement, expanded later using new technologies of light,^{5,6} electron (SEM),^{7–10} and transmission electron microscopy,^{11,12} have been extensively reviewed.^{13,14} However, the initial change in the thickness of PDL could not be identified because of technical difficulties. In a histological study, the thickness of the PDL is easily influenced by tissue preparation, such as handling, decalcification, and dehydration of the specimen.¹⁵ Furthermore, the number of histological sections is usually limited to a small number per tissue sample. In this way, it is usually not possible to obtain a fully three-dimensional (3D) view of tooth movement.

^a PhD student, Division of Orthodontics and Dentofacial Orthopedics, Nagasaki University Graduate School of Biomedical Sciences, Nagasaki, Japan.

^b Senior Assistant Professor, Division of Orthodontics and Dentofacial Orthopedics, Nagasaki University, Nagasaki, Japan.

^c Professor, Institute for Oral Science & High-Tech Center, Matsumoto Dental University, Shiojiri, Nagano, Japan.

^d Assistant Professor, Institute for Oral Science & High-Tech Center, Matsumoto Dental University, Shiojiri, Nagano, Japan.

^e Senior Assistant Professor, Division of Radiology and Cancer Biology, Nagasaki University, Nagasaki, Japan.

^f Assistant Professor, Division of Orthodontics and Dentofacial Orthopedics, Nagasaki University, Nagasaki, Japan.

^g Professor, Division of Orthodontics and Dentofacial Orthopedics, Nagasaki University, Nagasaki, Japan.

Corresponding author: Dr Hitoshi Hotokezaka, Division of Orthodontics and Dentofacial Orthopedics, Nagasaki University, Sakamoto 1-7-1, Nagasaki 852-8588, Japan. (e-mail: hotoke@nagasaki-u.ac.jp)

Accepted: September 2008. Submitted: July 2008.

© 2009 by The EH Angle Education and Research Foundation, Inc.

To assess the adaptive tissue response as a function of time, different animals had to be killed at different time intervals. It was not possible to monitor the in vivo adaptive response within the same animal. To overcome all these limitations, Arai et al¹⁶⁻¹⁸ developed a micro-CT system for in vivo animal imaging. This micro-CT system is characterized by high-resolution (voxel size of 0.125 mm), quick operation (exposure time, 17 s), low-radiation exposure (about 10 μ Sv/exposure) and can reproduce 0.02-mm slices.¹⁹

Orthodontic mesial tooth movement of the rat's upper first molar has been most frequently used to study the mechanisms of tooth movement and the response of periodontal tissues. However, the precise tooth movement has not been fully understood because it was difficult to evaluate using the previously available methods. In this study, we examined the rat's molar movement tridimensionally in individual living rats for a 28-day follow-up period by using an in vivo micro-CT. Furthermore, a finite element model (FEM) model of the rat's molar area was constructed, and tooth movement simulations with 10, 25, 50, and 100 g were performed.

MATERIALS AND METHODS

Twenty 10-week-old male young adult Wistar rats (SLC, Shizuoka, Japan; body weight, 230–250 g) were used as experimental animals. All rats were maintained under conventional conditions: 25°C \pm 2°C, 55% \pm 5% humidity, and 12-hour light-dark cycle. The rats were fed a commercial diet (MR Breeder, Nihon Nohsan Co, Kanagawa, Japan) and tap water ad libitum. All procedures for animal care were approved by the Animal Management Committee of the High-Tech Center of Matsumoto Dental University. The rats were divided into four groups of five rats each according to the magnitude of the applied force. Nickel-titanium closed-coil springs of 10, 25, 50, and 100 g (Sentalloy, Tomy Inc, Fukushima, Japan) were used to move the maxillary left molar mesially. The appliance was set under anesthesia (intraperitoneal injection of pentobarbital) with a dosage of 60 mg/kg body weight. The appliance set has been previously described²⁰ (Figure 1A,C,D).

Micro-CT (Rigaku Co, Tokyo, Japan) was taken under general anesthesia at day 0 (before and immediately after the appliance was set), 1, 2, 3, 10, 14, and 28 in the same animal (Figure 1B). Micro-CT settings were 100 kV and 160 μ A, with focus object distance of 74.8 mm, focus detector distance (FDD) of 498.8 mm, and image pixel size 30 \times 30 \times 30 μ m. Pixel size and pixel number were 480 \times 480 \times 480, field-of-view diameter was 14.4 mm, and height was 14.4

mm. Magnification was set at 6.7. At day 28, the rats were killed by CO₂ inhalation.

The image reconstruction at the appropriate cross section was carried out using i-VIEW software (J. Morita MFG Corp, Kyoto, Japan). Tooth movement was measured on the images using landmark points identified on the first molar's crown and roots (Figure 2A, left). The same investigator performed all measurements, and every measurement was repeated three times. The mean value was used as the final measurement. To assess measurement reproducibility, measurements were performed 10 times in one randomly selected rat root. The standard deviation was within 1%.

Measurement of Initial PDL Width Changes (0 to 3 Days)

Mesial and disto-buccal roots were divided into pressure and tension sides by the long axis of the roots. The mesial side was considered the pressure side, and the distal side was considered the tension side. The thickness of PDL was evaluated in the sagittal view by measuring the radiolucent area between the root and the alveolar bone. Point a was located in the apex of the root. Two parallel lines perpendicular to the long axis of the root divided the root into cervical and apical parts. In the mesial root pressure side, point b (apical) and point c (cervical) were registered. In the tension side, point d (apical) and point e (cervical) were recorded. Similarly, the disto-buccal root pressure side points g (apical) and h (cervical) and tension side points i (apical) and j (cervical) were measured. Point f was located in the apex of the root. Point m indicates tooth movement rate at the coronal level and was determined by the change in distance between the closest two points in the crowns of the first (M1) and second molar (M2) (Figure 2A, left).

Changes in the Vertical Plane (0, 10, 14, and 28 Days)

The changes in the vertical plane were measured at two sites: mesial and distal sulcus of the upper first molar in relation to the palatal plane. The palatal plane was defined as the line tangent to the lower border of the palatal vault (Figure 2A, right).

Angular Measurements

Changes in molar position were evaluated longitudinally by angular measurements (Figure 2B). The mesial root inclination angle was used to evaluate tooth movement in the sagittal plane. This angle was formed by the intersection of the long axis of the mesial root and the palatal plane. Disto-buccal and disto-palatal

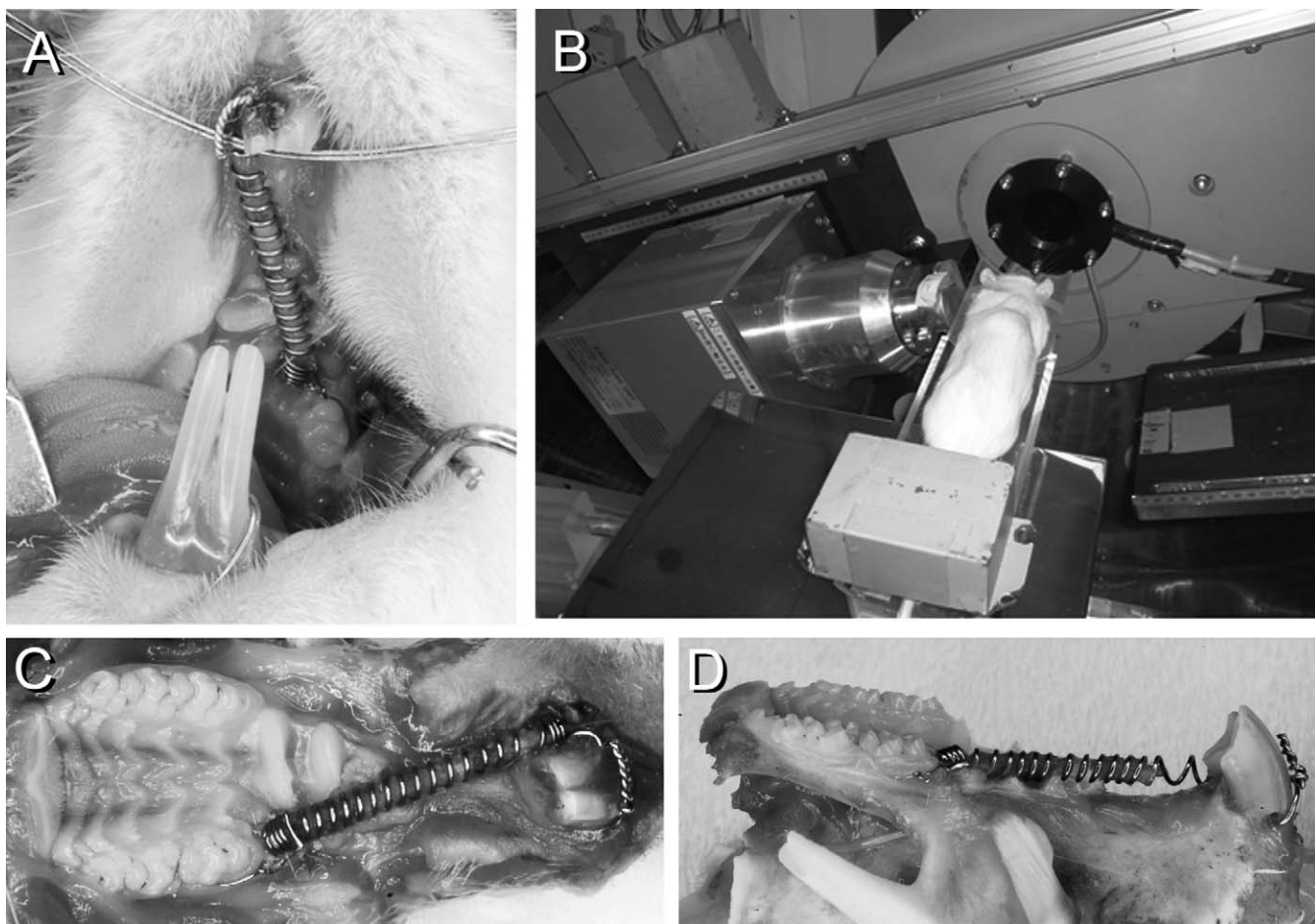


Figure 1. (A) Orthodontic appliance in situ. (B) An anesthetized rat set on the object stage of the micro-CT apparatus. Dissected rat maxilla with coil spring, occlusal (C) and lateral (D) views.

root-palatal plane angles evaluated the inclination of the molar in the coronal plane. These angles were formed by the intersection of the disto-buccal or disto-palatal root axis planes and the palatal plane. The axial rotation angle evaluated tooth movement in the axial plane. This angle was formed by two planes. One was the plane through the midpoints of the mesial and disto-buccal roots and the other the palatal suture.

Finite Element Method

We constructed a 3D FEM of the region of the maxillary molar, which consisted of 22,500 isoparametric tetrahedral-node solid elements and 4666 nodes (Table 1). Our model was created from micro-CT images of one rat using Mimics 11.11 (Materialise Software, Leuven, Belgium), Marc Mentat® software (MSC Software Corp, Santa Anna, Calif), and Patran™ 2007 r2 (MSC Software Corp). The geometry of the model was based on the measurements from micro-CT images taken from the control molars. The width of the PDL was set at 0.2 mm. Young's modulus of the tooth,

PDL, and bone were assumed to be 19,600 MPa, 0.7 MPa, and 13,700 MPa, respectively. Poisson ratio of the tooth, PDL, and bone were 0.15, 0.49, and 0.15, respectively. The mechanical properties of the PDL, tooth, and alveolar bone are indicated in Table 1B. To simulate orthodontic loads 10-, 25-, 50-, and 100-g forces were applied in the same direction of the in vivo orthodontic force. Movement was suppressed in 6 degrees of freedom for the nodes on the bottom edge of the alveolar bone. Tooth displacement and stress distribution analyses were performed using Marc® software (MSC Software Corp).

3D Superimposition

To visualize final tooth movements, 3D superimpositions were performed at day 28. The contours of the clinical crowns of the upper second and third molars were superimposed on those of the second and third molars from a pretreatment micro-CT image using commercial software (Imageware 9, UGS PLM Solutions, Plano, Texas). The superimposing method has

Table 1A. Element and Node Number

Material	Element	Node
Tooth	5004	845
Periodontal ligament	3323	1146
Alveolar bone	14,173	2675
Total	22,500	4666

been previously described.²¹ The superimpositions were performed within the same rat's material.

Statistics

Statistical analysis was performed with SPSS version 16.0 (SPSS, Chicago, Ill). The data were subjected to analysis of variance followed by Bonferroni adjustments for multiple comparisons among groups of rats.

RESULTS

The 3D reconstructed images showed the molar region and its surrounding bone. The PDL was observed as a radiolucent band between dentine and bone. The longitudinal evaluation of control molars (no tooth movement) indicated that the thickness of the PDL was not uniform (mean = 0.15 mm).

Initial PDL Changes

Point a indicated an intrusion movement of the mesial root at day 1. The evaluation of the pressure side of mesial roots showed a reduction of the PDL width at the cervical portion of the root (point c), whereas at the apical portion of the root (point b), the PDL width increased. In the tension side, the opposite picture was observed. There was an increase in the PDL width at the cervical portion of the root (point e) and a diminution of PDL width at the apical part of the root (point d). In the distal root, point f indicated an extrusion movement of the root. The PDL width was reduced in the pressure side (points g, h), while an increase was observed at points i and j (tension side; Figure 3).

Tooth Movement

At day 0, 1 hour after the coil spring was set, small tooth movement was observed. From day 1 to day 10, the amount of tooth movement gradually increased for all groups of forces. At day 14, there was a remarkable increase in tooth displacement when 10 g of force was applied. At day 28, tooth movement increased by more than two-fold in the 10-g group (Figure 3).

Linear Changes in the Vertical Plane

The mesial sulcus distance decreased gradually with time, indicating an intrusion movement of mesial

Table 1B. Mechanical Properties

Material	Young's Modulus, MPa	Poisson Ratio
Tooth	19,600	0.15
Periodontal ligament	0.7	0.49
Alveolar bone	13,700	0.15

root. A statistical difference among groups was found at day 28 when 50 and 100 g of force was applied (Figure 4A). The distal sulcus distance slightly decreased with time, indicating an intrusion movement of the distal roots. This trend was observed in all groups except for the 10-g group, which showed an abrupt increase in this measurement after 14 days. This suggests that 10 g of force application caused a different pattern of tooth movement: extrusion of the distal roots (Figure 4B).

Angular Measurements

The mesial root-palatal plane angle did not show any significant change when 25, 50, and 100 g of force were applied. However, at day 28, the 10-g-force group showed an increase in this angle, indicating mesial tipping of the molar. The axial rotation angle indicated that the molar had a slight mesial rotation tendency that increased with time. The disto-buccal root-palatal plane angle and the disto-palatal root-palatal plane angle showed almost the same trends because the roots are parallel with each other. However, the 10-g group showed a remarkable decrease in both angles, indicating more palatal inclination when compared with the rest of the groups (Figure 5).

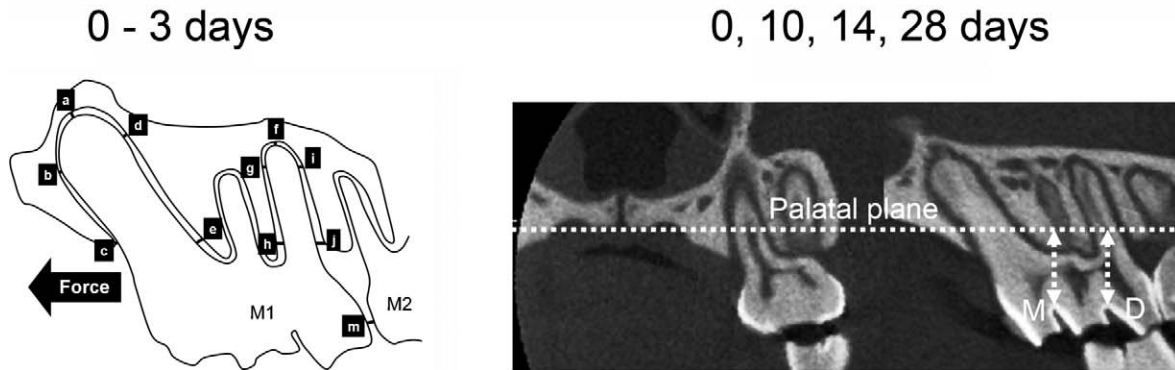
FEM

FEM analysis revealed that the major stress was produced on the cervical part of the disto-buccal root while the secondary stress was produced on the middle part of the mesial root (Figure 6). The root surface curves of maximum stress indicated that the magnitude of stress distribution was dependent on force magnitude. The simulation of the initial displacement of the molar immediately after orthodontic load showed a complex molar movement. Mesial and palatal tipping movement occurred simultaneously with intrusion of mesial root and extrusion of distal roots. The results were in agreement with the 3D superimposition (Figure 8). Furthermore, the center of rotation of the maxillary upper first molar was located in the center of five roots (apical third; Figure 7).

DISCUSSION

The clinical picture of orthodontic tooth movement consists of three phases: an initial and almost instan-

A. Linear measurements



B. Angular measurements (0, 10, 14, 28 days)

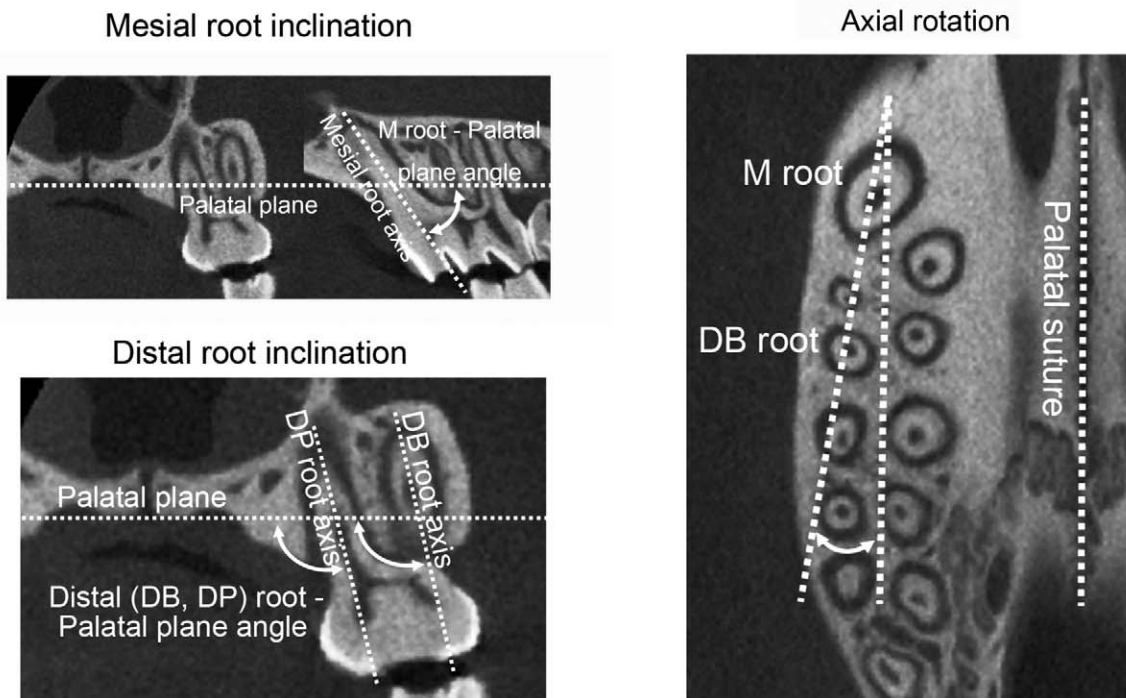


Figure 2. (A) Linear measurements. Left: reference points a, b, c, d, e, f, g, h, i, j, and m are indicated. Right: M, mesial, and D, distal sulcus. (B) Angular measurements. Left: upper, mesial root inclination angle; lower, disto-buccal and disto-palatal axis planes were measured in relation to the palatal plane. Right: axial rotation angle.

taneous tooth displacement; delay, during which no visible movement occurs; and a period of linear tooth movement.²²

Our results confirm the classical knowledge that when an orthodontic force is applied, tooth movement occurs in the direction of the force, by narrowing the PDL at the site of compression, with subsequent resorption of the alveolar bone. A widened PDL on the tension side indicates some kind of bone apposition.

These changes in the PDL thickness were found until day 3. From day 10, the PDL regained its normal width. For this reason, we evaluated tooth movement by measuring angles at day 0, 10, 14, and 28. From day 1 until day 3, a slight increase in tooth movement was observed. From day 3 to day 10, the lag period was observed in all force magnitudes, showing relatively low rates of tooth displacement or no displacement. It has been suggested that the lag phase is pro-

Linear measurements (0 - 3 days; mm)

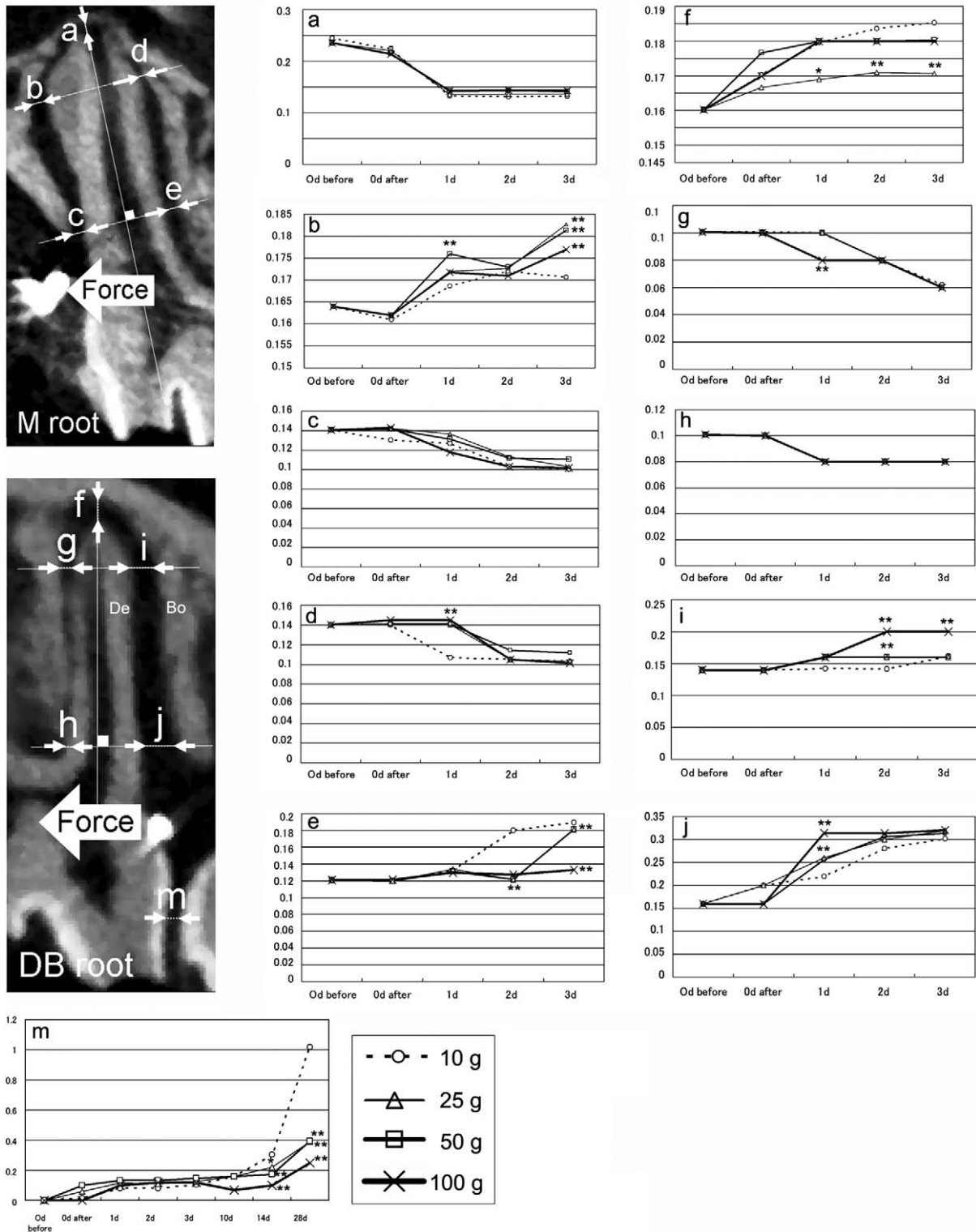
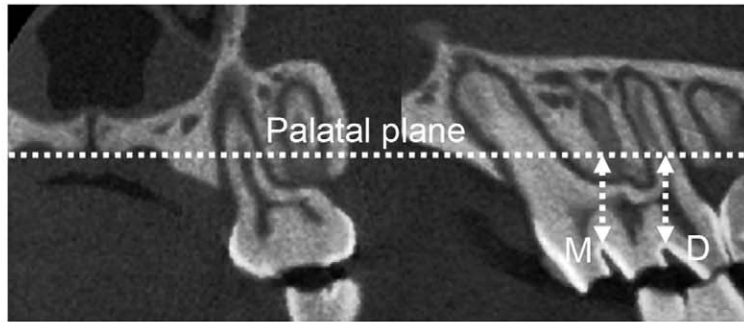
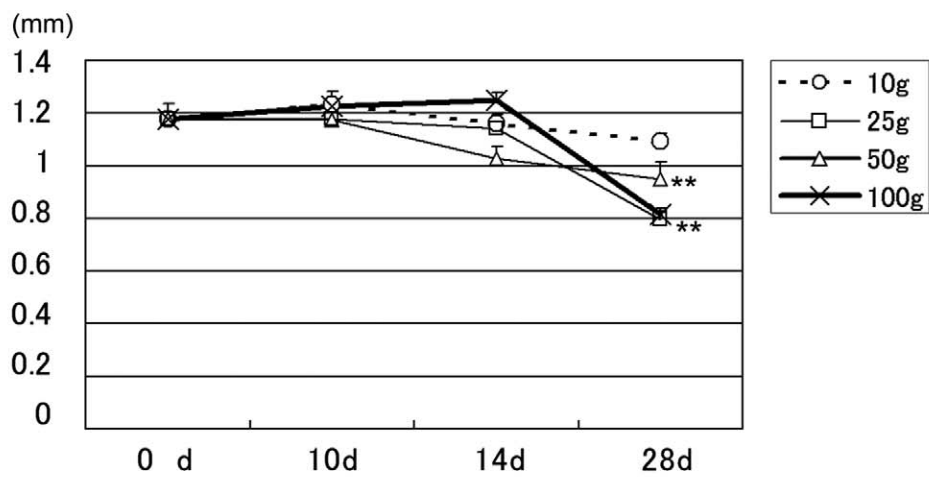


Figure 3. Left: micro-CT reconstructed images of mesial (M) and disto-buccal (DB) roots. These images were defined as planes through the center of mesial and disto-buccal roots perpendicular to the palatal plane and parallel to the palatal suture. The PDL was observed as the radiolucent area between dentine (De) and bone (Bo). Initial changes in the thickness of the PDL were measured at points a, b, c, d, e, f, g, h, i, j, and m. * $P < .05$; ** $P < .03$ compared with 10 g.

Changes in the vertical plane



A. Mesial sulcus - Palatal plane distance



B. Distal sulcus - Palatal plane distance

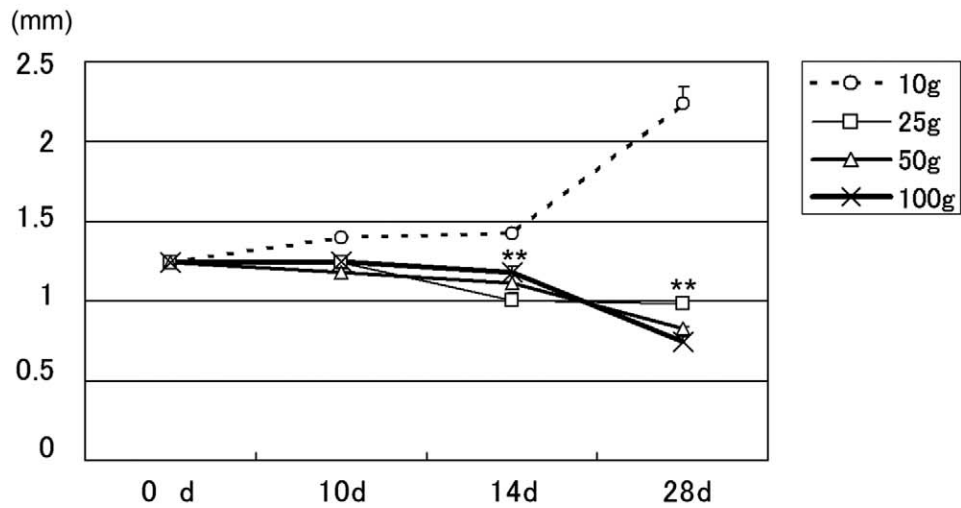


Figure 4. M, mesial, and D, distal sulcus, distance was measured in relation to the palatal plane. * $P < .05$; ** $P < .03$.

Angular measurements (0, 10, 14, 28 days; degrees)

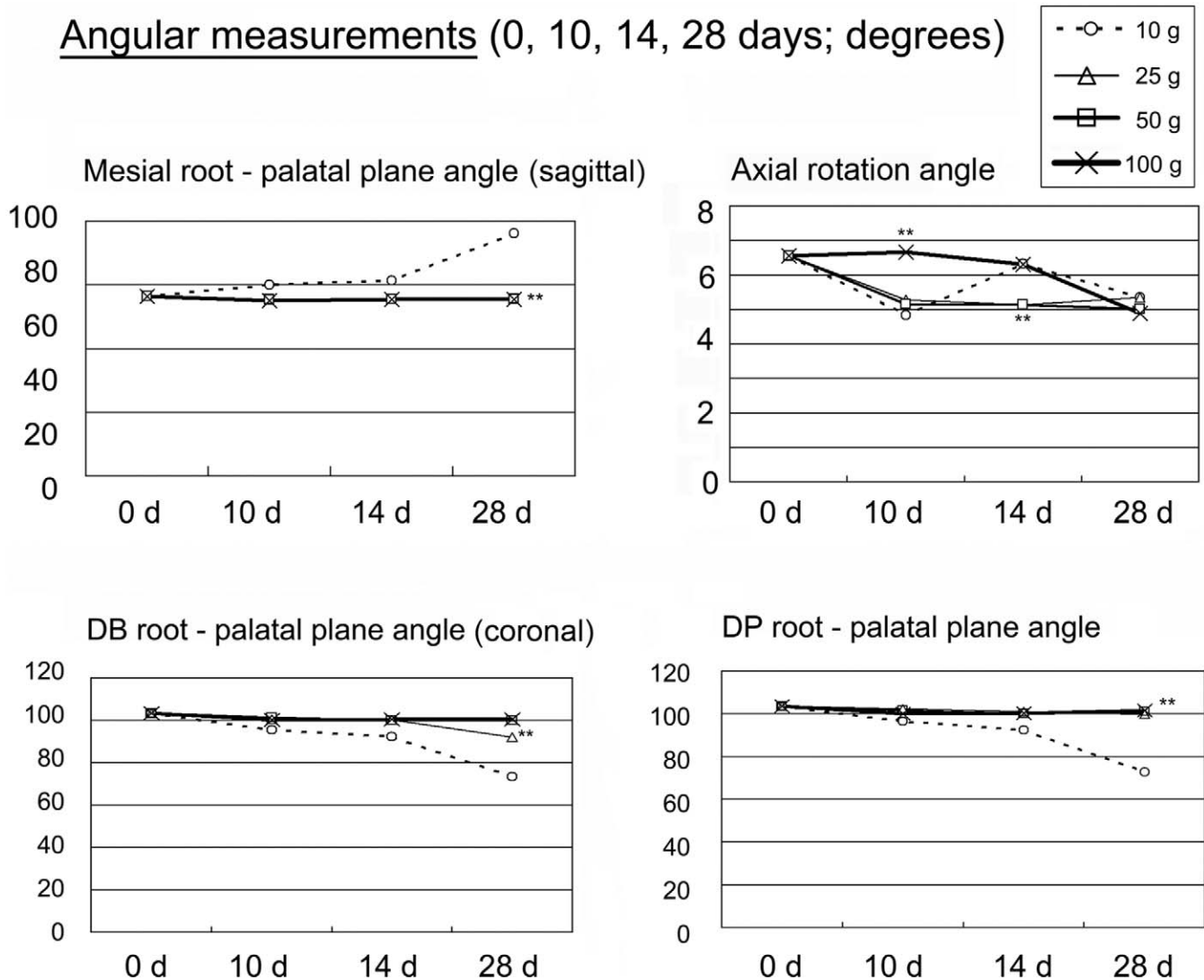


Figure 5. Mesial, disto-buccal (DB), and disto-palatal (DP) root-palatal plane and axial rotation angle measurements are shown. * $P < .05$; ** $P < .03$ compared with 10 g.

duced by hyalinization of the PDL in areas of compression.^{23,24} No further tooth movement occurs until cells complete the removal of all necrotic tissues.²⁵

After the lag period, the rate of movement gradually increased until day 28 when 25, 50, and 100 g were applied. However, 10-g force application showed a two-fold tooth movement rate from day 14 to day 28. This could be because the 10-g force application was the lightest force used in this study. As Sandstedt² postulated more than a century ago, when heavy forces are used, the PDL is overcompressed at first on the side of pressure and the underlying bone is not resorbed because of an apparent loss of tissue vitality.² Instead, undermining resorption occurs in the neighboring marrow spaces of the alveolar bone, and subsequently the bone and the compressed soft tissue in the region of the greatest pressure are removed.

When all the necrotic material is removed, the tooth assumes a new position. This interesting biologic reaction of the alveolar bone explains the fact that even by using heavy forces, orthodontic results are also obtained.

As tooth movement in rat molar is produced by a single force, our results may differ from orthodontic treatment in humans. To clarify a complex variety of force systems, further investigation is still needed.

CONCLUSIONS

- Longitudinal evaluation of tooth movement by in vivo micro-CT revealed the precise 3D motion; mesial inclination, extrusion of distal roots (disto-buccal and disto-palatal), intrusion of mesial root, slight palatal inclination, and mesial rotation of the molar.

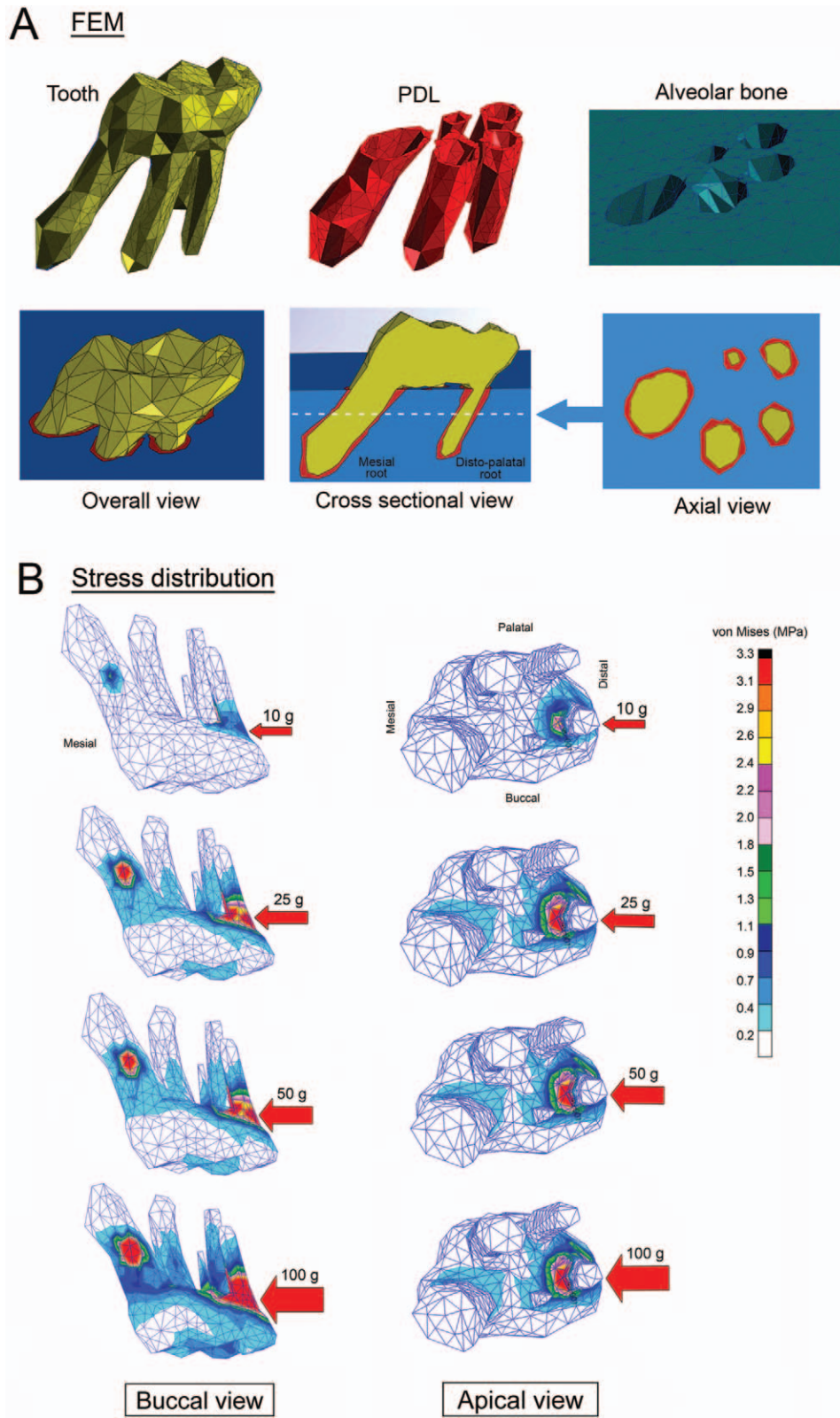


Figure 6. (A) Visualized finite element model. (B) Von Mises stress distribution in the periodontal ligament with different force magnitudes.

Molar displacement and center of rotation

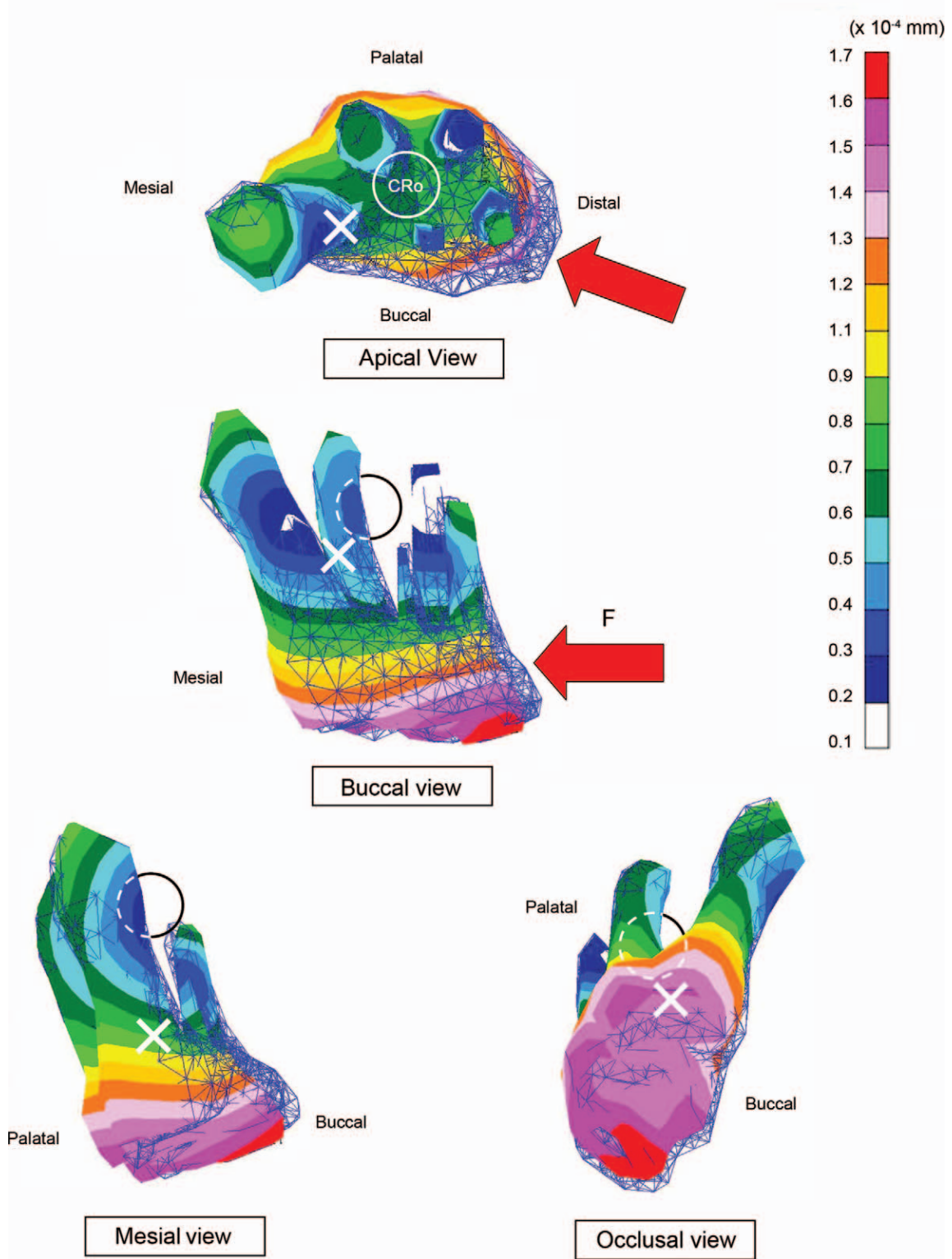
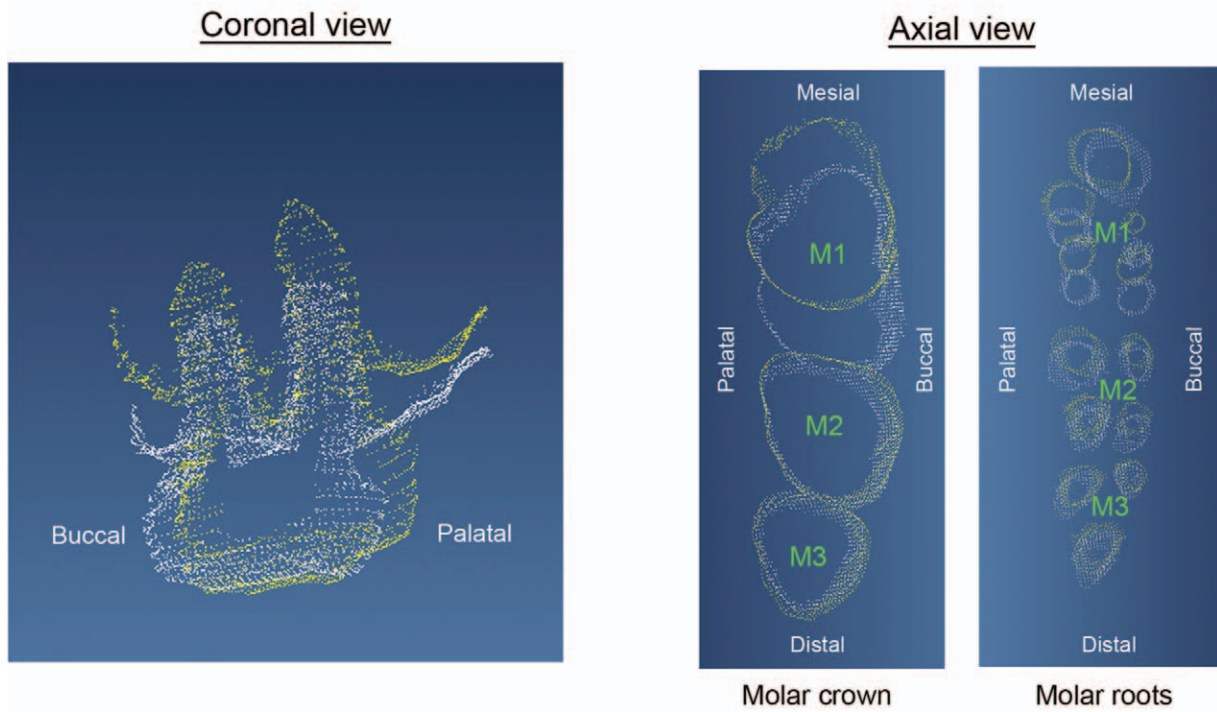


Figure 7. Molar displacement immediately after 100-g force application is shown by color contours. The tooth movement was magnified 1000 times. The initial position of the molar is indicated in dark blue (frame wire silhouettes). Circle CRo, center of rotation. X, center of resistance.

3D superimposition



Sagittal view

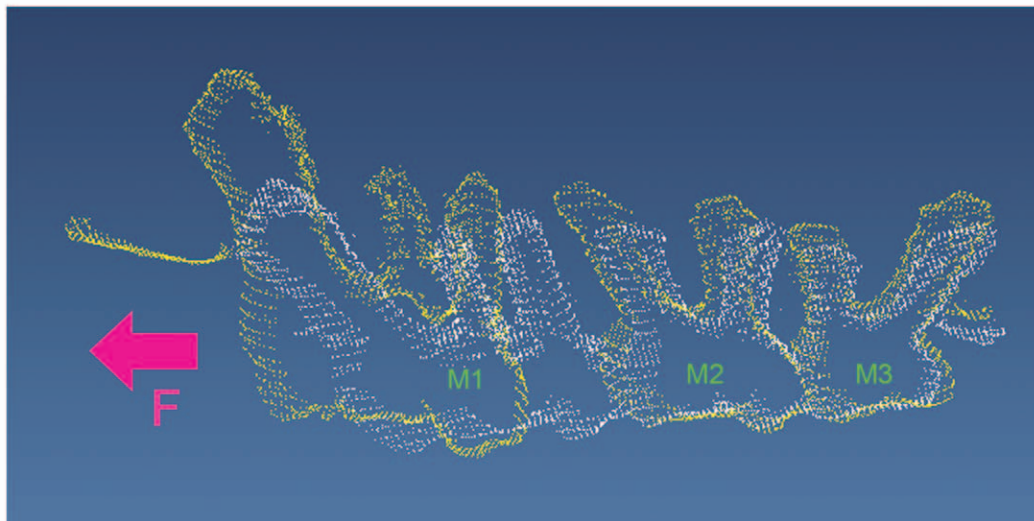


Figure 8. The applied force was 10 g. M1, M2, and M3 indicate first, second, and third molar, respectively. The white color represents pretreatment. Tooth movement after 28 days is shown in yellow.

- Although the initial tooth movement after the application of different force magnitudes until day 3 was not remarkably different, 10 g of force produced more tooth movement compared with heavier forces at day 28.

ACKNOWLEDGMENTS

This work was supported by a grant-in-aid for scientific research from the Ministry of Education, Science, Sports, and Culture of Japan. We thank the staff of the High-Tech Center of Matsumoto Dental University for their support during the experiments. Thanks are also extended to my colleagues in the Department of Orthodontics for their valuable help and assistance in this study.

REFERENCES

1. Proffit W. *The Biologic Basis of Orthodontic Therapy: Contemporary Orthodontics*. 3rd ed. St Louis, Mo: CV Mosby; 2000.
2. Sandstedt C. Contributions to the theory of orthodontic tooth movement. *Tandl Tidsskr*. 1904;5:236–256.
3. Oppenheim A. Tissue changes, particularly of the bone, incident to tooth movement. *Am Orthod*. 1911;3:57–67.
4. Schwarz A. Tissue changes incident to orthodontic tooth movement. *Int J Orthod*. 1932;18:331–352.
5. Reitan K, Kvam E. Comparative behavior of human and animal tissue during experimental tooth movement. *Angle Orthod*. 1971;41:1–14.
6. Storey E. The nature of tooth movement. *Am J Orthod*. 1973;63:292–314.
7. Rygh P. Ultrastructural changes in tension zones of rat molar periodontium incident to orthodontic tooth movement. *Am J Orthod*. 1976;70:269–281.
8. Roberts WE, Chamberlain JG. Scanning electron microscopy of the cellular elements of rat periodontal ligament. *Arch Oral Biol*. 1978;23:587–589.
9. Kvam E. Scanning electron microscopy of tissue changes on the pressure surface of human premolars following tooth movement. *Scand J Dent Res*. 1972;80:357–368.
10. Kvam E. Organic tissue characteristics on the pressure side of human premolars following tooth movement. *Angle Orthod*. 1973;43:18–23.
11. Grevstad HJ. Experimentally induced resorption cavities in rat molars. *Scand J Dent Res*. 1987;95:428–440.
12. Brudvik P, Rygh P. Non-clast cells start orthodontic root resorption in the periphery of hyalinized zones. *Eur J Orthod*. 1993;15:467–480.
13. Meikle MC. The tissue, cellular, and molecular regulation of orthodontic tooth movement: 100 years after Carl Sandstedt. *Eur J Orthod*. 2006;28:221–240.
14. Krishnan V, Davidovitch Z. Cellular, molecular, and tissue-level reactions to orthodontic force. *Am J Orthod Dentofacial Orthop*. 2006;129:e461–e432.
15. Nakamura Y, Noda K, Shimoda S, et al. Time-lapse observation of rat periodontal ligament during function and tooth movement, using microcomputed tomography. *Eur J Orthod*. 2008;30:320–326.
16. Arai Y, Ninomiya T, Tanimoto H. Development of in vivo micro computed tomography using flat panel detector. *Dentistry in Japan*. 2007;43:109–111.
17. Arai Y, Tammsialo E, Iwai K, Hashimoto K, Shinoda K. Development of a compact computed tomographic apparatus for dental use. *Dentomaxillofac Radiol*. 1999;28:245–248.
18. Arai Y, Yamada A, Ninomiya T, Kato T, Masuda Y. Micro-computed tomography newly developed for in vivo small animal imaging. *Oral Radiol*. 2005;21:14–18.
19. Nakajima A, Murata M, Tanaka E, et al. Development of three-dimensional FE modeling system from the limited cone beam CT images for orthodontic tipping tooth movement. *Dent Mater J*. 2007;26:882–891.
20. Gonzales C, Hotokezaka H, Yoshimatsu M, Yozgatian JH, Darendeliler MA, Yoshida N. Force magnitude and duration effects on amount of tooth movement and root resorption in the rat molar. *Angle Orthod*. 2008;78:502–509.
21. Jang I, Tanaka M, Koga Y, et al. A novel method for the assessment of three-dimensional tooth movement during orthodontic treatment. *Angle Orthod*. In press.
22. Wise GE, King GJ. Mechanisms of tooth eruption and orthodontic tooth movement. *J Dent Res*. 2008;87:414–434.
23. Brudvik P, Rygh P. Root resorption beneath the main hyalinized zone. *Eur J Orthod*. 1994;16:249–263.
24. Brudvik P, Rygh P. Multi-nucleated cells remove the main hyalinized tissue and start resorption of adjacent root surfaces. *Eur J Orthod*. 1994;16:265–273.
25. Reitan K. Effects of force magnitude and direction of tooth movement on different alveolar bone types. *Angle Orthod*. 1964;34:244–255.